

OPEN

# Shear Induced Interactions Cause Polymer Compression

Dave E. Dunstan\* & Dalton J. E. Harvie

**Shear induced particle pressure occurs in concentrated suspensions of particles. Importantly, the significance of the shear induced particle pressure has not been recognized in polymer rheology. The shear induced particle pressure results in an inward pressure on the polymer chains resulting in a shear dependent compressive force. The analytical form of the force balance equations that incorporate the effect of shear induced particle pressure predict a reduced polymer blob size and reducing viscosity with increasing shear rate as has been observed experimentally. Power law behavior is found for the viscosity in accord with the general observations for concentrated polymer rheology.**

Polymer dynamics is of wide practical importance and fundamental interest<sup>1</sup>. The models developed to describe polymer chains and their dynamics in flow derive from statistical mechanics and have the capacity to describe polymeric material mechanical properties<sup>2–6</sup>. An elegant connection between molecular properties and the macroscopic behavior has resulted<sup>1</sup>.

A generally accepted assumption of the field is that the polymer chains extend in flow due to the hydrodynamic forces on the chains<sup>4</sup>. Kuhn was the first to propose the dumbbell model that is used in most of the current modelling of polymers in flow in order to directly relate the macroscopic properties of the polymers in flow to the single chain physics<sup>7</sup>. The dumbbell model, in which the polymers are modelled as two beads on an elastic (generally Hookean) FENE spring, is still used in modified forms as it is thought to encapsulate the key physics of the macromolecules in flow<sup>8</sup>. Physically, a dumbbell experiences two Stokes drags during shear that cause extension and compression as the dumbbells precess in Jeffrey orbits<sup>9</sup>, however the constitutive dumbbell models do not incorporate these orbits, instead they predict polymer extension<sup>8</sup>. Kuhn also developed a statistical mechanical model to predict the Hookean force law for the ideal chains that acts as a restoring force to counter the hydrodynamic forces<sup>10</sup>. Kuhn initially assumed that the dumbbell could either extend or compress in flow as it rotates around the vorticity axis.

Kuhn and Grun (1942) published the first paper to assume that the chains only extend in simple flow<sup>11</sup>. Essentially, they assumed that only extension occurs and ignored Kuhn's original insight that the chains would undergo both compression and extension in simple flow. By assuming that only extension occurs, the relationship between the reduced shear rate and the end-to-end vector of the chains was calculated. The reduced extension versus shear rate shows a limiting extension at high shear rates<sup>11</sup>.

Cottrell, Merrill and Smith reported the first measurement of light scattering from polymer solutions in shear in 1969<sup>12</sup>. More recently Link and Springer<sup>13</sup> and then Lee, Solomon and Muller<sup>14</sup> measured light scattering on polymer solutions in Couette flow<sup>15</sup>. Generally, the interpreted deformation is significantly less than the Rouse and Zimm models predict<sup>16,17</sup>. The observed behaviour may also be interpreted as being due to the orientation of the random ensemble of prolate chains in the flow field without the need to invoke any extension of the chains<sup>14,18,19</sup>. The overall shear induced orientation of the prolate chains, in Jeffrey orbits, increases the scattering cross section in the direction perpendicular to the vorticity axis and along the flow direction. This results in an apparent extension parallel to the flow and compression perpendicular to the flow direction. In the quiescent state the solution appears isotropic due to the random orientation of the prolate chains, then becomes anisotropic in flow via the orientation of the chains. Rheo-optic measurements on dilute solutions of polydiacetylenes in Couette flow show increased projection of the chains in the flow direction, with no deformation of the backbone<sup>14</sup>.

Fluorescently labelled DNA in flow has also been experimentally examined by a number of researchers. The first papers in the field were by Smith, Babcock and Chu<sup>19</sup> and in the same year Le Duc, Haber, Bao and Wirtz who used confocal fluorescence microscopy to directly image labelled DNA in Couette flow<sup>20</sup>. In both works the DNA was visualised using fluorescence microscopy with sliding plates to generate Couette flow and maintain the DNA molecules in the field of view. The DNA is claimed to be representative of random chain polymers in solution. The images show a macroscopic “blob” of several segment lengths that does not appear completely representative of a random chain polymer. Simply, the DNA images are not of a random chain whose conformation

Department of Chemical Engineering, University of Melbourne, VIC, 3010, Australia. \*email: [davided@unimelb.edu.au](mailto:davided@unimelb.edu.au)

is determined by entropy<sup>19,20</sup>. Furthermore, the resolution of the microscopy method determines that compression is difficult to observe<sup>19</sup>. Larson has written a comprehensive review of the rheology of dilute solutions of flexible polymers focusing on the progress and problems<sup>21</sup>. A considerable component of the review is focused on simulations and modelling the data obtained from DNA. A key conclusion is that the measured deformation is less than expected. It should be noted that DNA does not show the same rheological behaviour as that observed for typical random coil polymers. Typical random coil polymers have conformation that is determined by their entropy and show decreasing viscosity with increasing shear rate and increasing temperature<sup>22,23</sup>. Calf thymus DNA shows decreasing viscosity with shear rate and increasing viscosity with temperature<sup>23</sup>. A recent study by Bravo-Anaya *et al.* interprets the observed rheological behaviour as resulting from interacting aggregates of the DNA molecules in flow<sup>22</sup>. The interaction between the DNA molecules is suggested to be driven by H-bonding. In summary, the evidence for polymer chain extension in simple flow at high concentrations above critical overlap is less than compelling.

Since Kuhn's original paper, the possibility of compression in Couette flow has not been considered and only extension has been assumed in the field<sup>4,6,8,24–26</sup>. However, recent experimental evidence has shown chain compression in Couette flow at semi-dilute concentrations<sup>27–29</sup>.

Rheo-optical measurements on synthetic polymers have shown chain orientation in dilute solution and compression at concentrations above critical overlap in the semi-dilute region<sup>14,28,30</sup>. These experimental results have prompted a revision of the idea of extension being a universal assumption for polymers in simple planar flow. An alternative approach that assumes compression, allows the measured radius-shear rate behaviour to be predicted, and the power law behaviour observed for polymers in flow to be modelled<sup>29</sup>. Furthermore, using a force balance argument that predicts the shear thinning rheological behaviour, also enables the viscosity-radius relationship to be predicted. The predicted power law behaviour of the viscosity-radius is in close agreement with the experimentally observed behaviour<sup>29,31</sup>. Interestingly, this shows that the viscosity decreases as the radius decreases in a manner that is physically consistent with the observed behaviour for concentrated random chain polymers<sup>29</sup>. The generally observed decrease in viscosity with increasing temperature for polymer solutions and melts has been attributed to coil compression. The decreasing viscosity with increasing shear rate has been assumed to result from coil extension. This apparent physical inconsistency is resolved if the coils are assumed to compress with increasing shear rate<sup>31</sup>.

It is also worth noting that Frith *et al.*<sup>32,33</sup> showed that for sterically stabilized particles with a “soft” stabilizing layer that the stabilizing chains are observed to compress with increasing concentration and shear rate. This is strong evidence that the compressive shear induced particle pressure results in a shear dependent compressive force on the chains.

Models of shear induced particle pressure have been developed by a number of researchers. Notably, Nott and Brady and a number of key papers by Morris and co-workers have added new insight into the rheology of concentrated suspensions<sup>34–39</sup>. The 2009 review by Morris gives an elegant overview of the development of the field<sup>39</sup>. The first experimental determination of the shear induced particle pressure was by Bagnold in 1954 who suggested the idea of a particle pressure under shear in order to explain his observations<sup>40</sup>. The experimental understanding was further developed by Deboeuf *et al.* in an elegant work where the suspension was placed in a Couette cell and the change in pressure directly measured as a function of the shear rate and volume fraction<sup>36</sup>. The shear induced particle pressure was found to be a linear function of the shear rate and the square of the volume fraction of the suspension.

Particles in solution experience at least two additional compressive normal stresses, or pressures, in addition to the hydrodynamic pressure existing in the solute. The random Brownian motion of the particles causes collisions (or interactions) between particles (in addition to solute interactions which are captured by the hydrodynamic pressure), and on average these interactions create a compressive normal stress on the particle: the osmotic pressure. Particle pressure is the second additional pressure, and is similar to osmotic pressure but instead is a result of the shear induced motion of the particles. The particle pressure increases as the collisional frequency increases when the suspension is exposed to a shear stress<sup>34,35,41</sup>. The increased collisional frequency results in an increased inward pressure on the particle: the particle pressure. The rheology of dense suspensions is reviewed by Guazzelli and Pouliquen<sup>42</sup>. Further modelling has been undertaken by Rampall *et al.* and later Wilson *et al.* for spheres with surface roughness<sup>43–45</sup>.

## Theory

Herein we develop a model that incorporates the shear induced particle pressure for polymer blobs in flow to predict how the polymer radius, and hence shear viscosity of the suspension, scales as a function of shear rate. The polymers are treated as spherical, porous, elastic particles at concentrations above critical overlap where the excluded volume terms may be neglected<sup>2–4</sup>. It is also assumed that the chains are not entangled. These assumptions are in accord with the Rouse model that ignores both entanglements and hydrodynamic interactions<sup>16,46,47</sup>.

The application of an anisotropic shear stress (Couette flow) causes collisions between the particles that results in a compressional stress being applied to the polymers at a local level. The normal stresses realized in the three directions are given as the diagonal components of the particle stress tensor<sup>40</sup>. In general these components are different in magnitude, however, they all have the same sign, meaning that they all act to compress the particles in suspension<sup>35</sup>. The particle pressure is defined as the average diagonal (isotropic) component of the particle stress tensor. In our analysis we assume that particle compression is a function of this average isotropic stress, or particle pressure<sup>36,39</sup>. Here the form of the particle interaction pressure developed by Brady and Morris<sup>35</sup> and others<sup>38,48</sup> for concentrated suspensions means that the particle interaction stress scales as:

$$\sigma_H \sim \eta_n \dot{\gamma} \quad (1)$$

here the viscosity,  $\eta_n$ , is representative of the normal stresses developed in the suspension (proportional to  $\phi^2$  to leading order), and  $\dot{\gamma}$  is the shear rate.

The shear induced interaction stress on the polymers that compresses the blobs is balanced by the elastic restoring force in each chain. Given that the concentration is assumed to be above critical overlap, the excluded volume and osmotic stresses in the system will be uniform, isotropic and constant (independent of shear stress). The elastic stress resulting from the chain deformation may then be written;

$$\sigma_{el} = -\frac{\partial F_{el}}{\partial V} = \frac{9k_B T}{8\pi R_0^2 R} \quad (2)$$

where  $F_{el}$  is the elastic free energy of the chain,  $k_B$  Boltzmann's constant,  $T$  the absolute temperature,  $R_0$  the unperturbed chain radius,  $R$  the radius of the chain in flow and  $V$  the volume of the chains.

Equating the elastic and interaction stresses at steady state yields:

$$R \sim \frac{k_B T}{\eta_n \dot{\gamma}} \quad (3)$$

To find the particle radius and shear viscosity we represent the shear and normal viscosities by

$$\begin{aligned} \eta_s &\sim \phi^{n_s} \\ \eta_n &\sim \phi^{n_n} \end{aligned} \quad (4)$$

where the  $n_s$  and  $n_n$  are viscosity volume fraction exponents corresponding to shear and normal directions. Substitution of the form of Equations [4] in equation [3], and noting that  $\phi \sim R^3$ , yields:

$$R \sim \dot{\gamma}^{-\frac{1}{3n_n+1}} \quad (5)$$

and:

$$\eta_s \sim \dot{\gamma}^{-\frac{3n_s}{3n_n+1}} \quad (6)$$

In the simplest case of a semi-dilute solution of polymers, to leading order  $\eta_n \sim \phi^2$ , the radius scales with shear as  $R \sim \dot{\gamma}^{-1/7}$  and the volume fraction by  $\phi \sim \dot{\gamma}^{-3/7}$ . Adopting a general power law for the shear viscosity of the solution, as per Equations [4], the shear viscosity then scales as  $\eta_s \sim \dot{\gamma}^{-\frac{3n_s}{7}}$ .

Alternatively, the viscosities appearing in Equations [4] may be assumed to be that of a suspension of particles, with relationships taken from the suspension literature. For example, Morris *et al.*<sup>38</sup> give:

$$\begin{aligned} \eta_n &= \eta_0 \frac{K_n \bar{\phi}^2}{(1 - \bar{\phi})^2} \\ \eta_s &= \eta_0 \left[ 1 + \frac{2.5 \phi_{\max}}{1 - \bar{\phi}} + \frac{K_s \bar{\phi}^2}{(1 - \bar{\phi})^2} \right] \end{aligned} \quad (7)$$

Boyer *et al.*<sup>49</sup> has given the same expressions with different  $K_n$  and  $K_s$  values. There are other relationships in the literature, but they all have a similar form that captures the experimentally observed trends. The viscosity exponents are plotted in Fig. 1. Importantly as  $\phi$  approaches the maximum packing limit, both viscosities scale in the same manner<sup>49</sup>. Physically this is reasonable given that both are determined by the collisional frequency between the blobs. The inset in Fig. 1 shows the behavior of the  $n_i$  values over the full range of volume fractions and that the values converge in the limit. We can express the relationships of Equation [7] in the form of Equations [4] by calculating effective exponents that vary with volume fraction, using  $n_i = \frac{d \ln(\eta_i)}{d \ln(\phi)}$  for  $i = n, s$ . These exponents, as well as the resulting radius and shear viscosity scalings (defined by  $\dot{\gamma}^{m_n}$  and  $\dot{\gamma}^{m_s}$ ) are plotted in Fig. 2 for the  $K_n$  and  $K_s$  values employed by Miller *et al.*<sup>50</sup>.

The form of the power law behavior then becomes a function of the concentration as the values of  $n_s$  and  $n_n$  both vary as shown in this figure and summarized in Table 1 below<sup>49</sup>.

The current work proposes that polymer compression in flow is a result of the shear induced particle pressure that acts to decrease the chain size with increasing shear rate. Rheo-optical measurements on several random chain polymers at concentrations in the semi-dilute regime have shown compression in flow<sup>31,51,52</sup>. Furthermore, power law behavior was observed with the decrease in chain radius with increasing shear rate. The predicted power law exponent with shear rate of  $-0.11$  obtained for PMMA<sup>52</sup> at a volume fraction of 0.24 is presented in Fig. 2, and shows very good agreement with the theoretical prediction of  $-1/7$ . Given that this theory has no adjustable parameters and that the experimental data has been previously published, this is significant. Furthermore, this suggests that the model captures the key physics of the problem. There have been several studies on polymer solutions in shear that indicate the presence of concentration fluctuations due to the imposition of shear<sup>46,53</sup>. The chain compression predicted in the current study is consistent with the models and experimental evidence collected for polymers in flow using light scattering<sup>54</sup>. In the limit of high concentration, the blobs are highly compressed in the quiescent state and therefore show no further reduction in size with imposed shear.

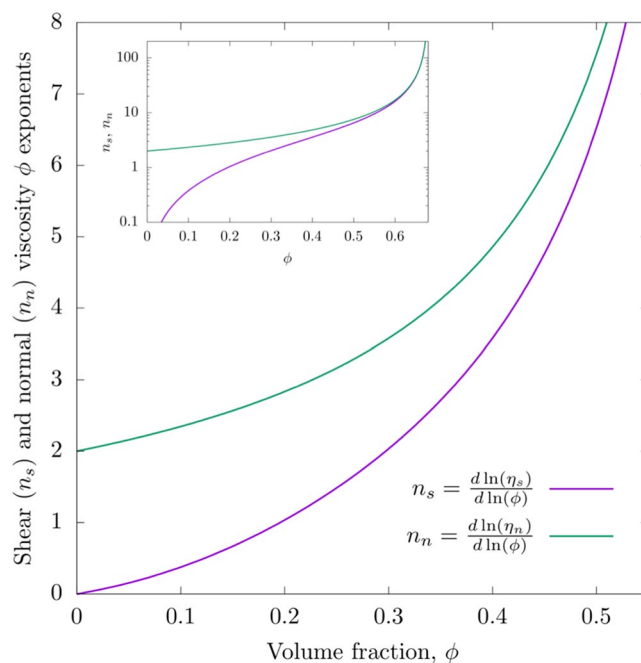


**Figure 1.** The volume fraction exponents plotted versus the volume fraction using Equation [7] based on values taken from Miller *et al.*<sup>50</sup>. Note that at high volume fraction the values of the normal and shear exponents converge as seen in the inset.

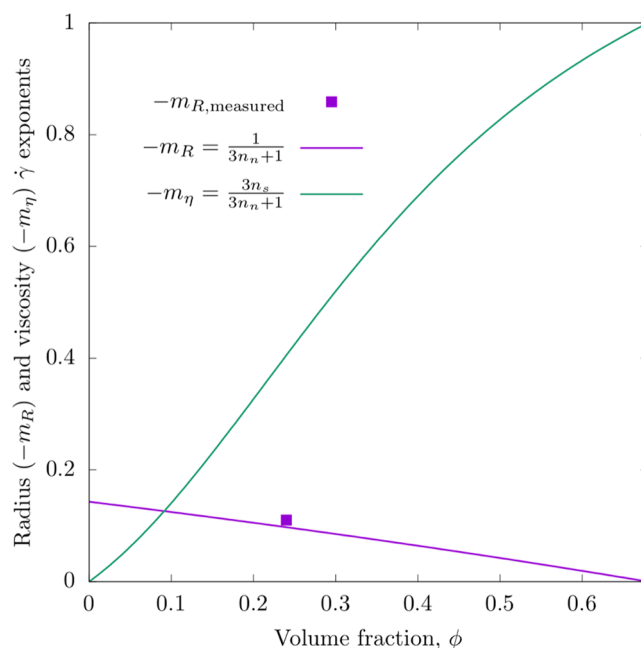


**Figure 2.** Plot of the shear rate exponents versus volume fraction for the viscosity and radius. Note that the viscosity exponent increases with volume fraction while the radius exponent decreases with volume fraction toward the limiting values of both at the limiting volume fraction. The experimental point is taken from ref. <sup>51</sup>.

The model developed here also predicts a power law for the shear thinning (viscosity-shear rate) behavior that is within the range (typically  $-0.5$  to  $-1.0$ ) observed for typical polymer systems<sup>55,56</sup>. Using the expression determined by Morris and Boulay<sup>38</sup> (for hard spheres) for the different concentration ranges (see Table 1) enables differing power law behaviours to be determined.

It should be noted that hard sphere systems have been shown to be effectively Newtonian for volume fractions of less than approximately  $0.3$ <sup>57</sup>. Thus, the values of the power law exponent found for the model indicate that the shear thinning in polymers is a result of chain compression at low volume fraction. The absence of shear thinning

Concentration Regime	Exponent Values	Viscosity-Shear rate relationship, $\dot{\gamma}^{m_{eta}}$	Radius Shear rate relationship, $\dot{\gamma}^{m_R}$
Dilute	$n_s = 0, n_n = 2$	$\eta_s \sim \dot{\gamma}^{-0} = 1$	$R \sim \dot{\gamma}^{-1/7}$
Semi-dilute	$n_s = 1, n_n = 2$	$\eta_s \sim \dot{\gamma}^{-3/7}$	$R \sim \dot{\gamma}^{-1/7}$
Concentrated	$n_s = n_n = n,$	$\eta_s \sim \dot{\gamma}^{-\frac{3n}{3n+1}}$	$R \sim \dot{\gamma}^{-\frac{1}{3n+1}}$
	$n \rightarrow \infty$	$\eta_s \sim \dot{\gamma}^{-1}$	$R \sim 1$

**Table 1.** Results of the predicted power law behavior for the viscosity and radius for the three different concentration regimes. The values of  $n_s$  and  $n_n$  for the different concentration regimes are taken from Boyer *et al.*<sup>49</sup>.

for hard spheres at low volume fractions also indicates that there is no structural rearrangement occurring in the suspensions. A detailed comparison of the polymer systems and hard sphere suspensions would allow the contributions of spatial rearrangement and ordering to be compared with the effect of chain compression. The model predicts the correct limiting behavior of the shear viscosity as being independent of the shear rate in dilute solution through to an inverse relationship in concentrated solutions. The model correctly covers the range of power laws observed for polymer solutions. In a future work, the power law behavior observed for polymers will be reviewed and compared with the model. However, the variation in the exponents of the shear and normal viscosities with volume fraction appears to predict the general behavior of polymers in flow.

## Conclusions

The shear induced particle pressure results in an overall compressive force on polymer chains in simple Couette flow. By assuming that the chains are permeable blobs and the shear induced pressure is isotropic, the chain size and solution viscosity power law behaviour may be predicted. Using the shear induced pressure and elastic restoring force enables the radius-shear rate power law of  $-1/7$  to a constant radius at high concentrations to be predicted while also yielding a power law exponent for the viscosity of  $-0.4$  that is within the range of exponents measured for polymer systems.

Received: 16 December 2019; Accepted: 11 March 2020;

Published: 26 March 2020

## References

- Sperling, L. H. *Introduction to Physical Polymer Science*. (Wiley Interscience: NJ 1992).
- Flory, P. J. *Statistical Mechanics of Chain Molecules*. (Hanser Publications: New York, 1988).
- Flory, P. J. *Principles of Polymer Chemistry*. (Cornell University Press, 1953).
- deGennes, P. G. *Scaling Concepts in Polymer Physics*. (Cornell University Press: Ithaca, 1979).
- Treloar, L. R. G. *The Physics of Rubber Elasticity*. (Oxford University Press, Oxford 1975).
- Doi, M. & Edwards, S. F. *The Theory of Polymer Dynamics*. (Clarendon Press: Oxford, 1986).
- Kuhn, W. Über quantitative Deutung der Viskosität und Strömungsdoppelbrechung von Suspensionen. *Kolloid Zeitschrift* **62**, 269–285 (1933).
- Bird, R. B., Curtiss, C. F., Armstrong, R. C. & Hassager, O. *Dynamics of Polymeric Liquids, Volume II, Kinetic Theory*. (Wiley-Interscience: New York, 1987).
- Jeffery, G. B. The motion of ellipsoid particles immersed in a viscous fluid. *Proceedings of the Royal Society of London Series A* **102**, 161–179 (1922).
- Kuhn, W. Über die gestalt fadenformiger molekule in losungen. *Kolloid Z.* **68**, 2–16 (1934).
- Kuhn, W. & Grün, F. Beziehungen zwischen elastischen konstanten und Dehnungsdoppelbrechung hochelastischer Stoffe. *Kolloid-Zeitschrift* **101**, 248–271, <https://doi.org/10.1007/bf01793684> (1942).
- Cottrell, F. R., Merrill, E. W. & Smith, K. A. Conformation of polyisobutylene in dilute solution subjected to a hydrodynamic shear field. *Journal of Polymer Science Part A-2: Polymer Physics* **7**, 1415–1434, <https://doi.org/10.1002/pol.1969.160070811> (1969).
- Link, A. & Springer, J. Light scattering from dilute polymer solutions in shear flow. *Macromolecules* **26**, 464–471, <https://doi.org/10.1021/ma00055a010> (1993).
- Gason, S. *et al.* Rheo-optical Studies of Polydiacetylene. *J. Phys. Chem. B* **101**, 7732–7735 (1997).
- Lee, E. C., Solomon, M. J. & Muller, S. J. Molecular Orientation and Deformation of Polymer Solutions under Shear: A Flow Light Scattering Study. *Macromolecules* **30**, 7313–7321, <https://doi.org/10.1021/ma9706945> (1997).
- Rouse, P. E. A Theory of the Linear Viscoelastic Properties of Dilute Solutions of Coiling Polymers. *J. Chem. Phys.* **21**, 1272–1280 (1953).
- Zimm, B. H. Dynamics of Polymer Molecules in Dilute Solution: Viscoelasticity, Flow Birefringence and Dielectric Loss. *J. Chem. Phys.* **24**, 269–278 (1956).
- Bruno, W. *Colloid Polym. Sci.* **254**, 325–328 (1976).
- Smith, D. E., Babcock, H. P. & Chu, S. Single-Polymer Dynamics in Steady Shear Flow. *Science* **283**, 1724–1727, <https://doi.org/10.1126/science.283.5408.1724> (1999).
- LeDuc, P., Haber, C., Bao, G. & Wirtz, D. Dynamics of Individual Flexible Polymers in a Shear Flow. *Nature* **399**, 564–566 (1999).
- Larson, R. G. The rheology of dilute solutions of flexible polymers: Progress and problems. *Journal of Rheology* **49**, 1–70, <https://doi.org/10.1122/1.1835336> (2005).
- Bravo-Anaya, L. M. *et al.* Supramolecular Organization in Calf-Thymus DNA Solutions under Flow in Dependence with DNA Concentration. *Macromolecules* **50**, 8245–8257, <https://doi.org/10.1021/acs.macromol.7b01174> (2017).
- Bravo-Anaya, L. M., Rinaudo, M. & Soltero-Martínez, F. A. Conformation and Rheological Properties of Calf-Thymus DNA in Solution. *Polymers* (20734360) **8**, 1–19, <https://doi.org/10.3390/polym8020051> (2016).
- Bird, B. B., Stewart, W. E. & Lightfoot, E. N. *Transport Phenomena*. (John Wiley, 2002).
- Bird, R. B., Armstrong, R. C. & Hassager, O. *Dynamics of Polymeric Liquids, Volume I, Fluid Mechanics*. (Wiley-Interscience: New York, 1987).

26. Rubinstein, M. & Colby, R. H. *Polymer Physics*. (Oxford University Press, 2003).
27. Chan, N. Y. C., Chen, M., Hao, X.-T., Smith, T. A. & Dunstan, D. E. Polymer Compression in Couette Flow. *J. Phys. Chem. Lett.* **1**, 1912–1916 (2010).
28. Dunstan, D. E., Hill, E. K. & Wei, Y. Direct Measurement of Polydiacetylene segmental Orientation and Deformation in Flow: semi-dilute Behaviour. *Macromolecules* **37**, 1663–1665 (2004).
29. Xie, D. & Dunstan, D. E. Modelling polymers as compressible elastic spheres in Couette flow. *Substantia* **1**, 43–47 (2017).
30. Chan, N. Y., Chen, M. & Dunstan, D. E. Elasticity of polymer solutions in Couette flow measured by fluorescence resonance energy transfer (FRET). *The European physical journal. E, Soft matter* **30**, 37–41 (2009).
31. Dunstan, D. E. The Viscosity Radius Relationship for Concentrated Polymer Solutions. *Scientific Reports* **9**, 1–9 (2019).
32. Frith, W. J., d’Haene, P., Buscall, R. & Mewis, J. Shear thickening in model suspensions of sterically stabilized particles. *Journal of Rheology* **40**, 531–548, <https://doi.org/10.1122/1.550791> (1996).
33. Mewis, J., Frith, W. J., Strivens, T. A. & Russel, W. B. The rheology of suspensions containing polymerically stabilized particles. *AIChE Journal* **35**, 415–422, <https://doi.org/10.1002/aic.690350309> (1989).
34. Nott, P. R. & Brady, J. F. Pressure-driven flow of suspensions: simulation and theory. *Journal of Fluid Mechanics* **275**, 157–199, <https://doi.org/10.1017/S0022112094002326> (1994).
35. Brady, J. F. & Morris, J. F. Microstructure of strongly sheared suspensions and its impact on rheology and diffusion. *J. Fluid Mech.* **348**, 103 (1997).
36. Deboeuf, A., Gauthier, G., Martin, J., Yurkovetsky, Y. & Morris, J. F. Particle Pressure in a Sheared Suspension: A Bridge from Osmosis to Granular Dilatancy. *Physical Review Letters* **102**, 108301, <https://doi.org/10.1103/PhysRevLett.102.108301> (2009).
37. Kulkarni, P. M. & Morris, J. F. Pair-sphere trajectories in finite-Reynolds-number shear flow. *J. Fluid Mech.* **596**, 413 (2008).
38. Morris, J. F. & Boulay, F. Curvilinear flows of noncolloidal suspensions: The role of normal stresses. *Journal of Rheology* **43**, 1213–1237, <https://doi.org/10.1122/1.551021> (1999).
39. Morris, J. F. A review of microstructure in concentrated suspensions and its implications for rheology and bulk flow. *Rheologica Acta* **48**, 909–923 (2009).
40. Bagnold, R. A. Experiments on a Gravity-Free Dispersion of Large Solid Spheres in a Newtonian Fluid under Shear. *Proceedings of the Royal Society of London. Series A, Mathematical and Physical Sciences* **225**, 49–63 (1954).
41. Brady, J. F. & Bossis, G. The rheology of concentrated suspensions of spheres in simple shear flow by numerical simulation. *Journal of Fluid Mechanics* **155**, 105–129, <https://doi.org/10.1017/S0022112085001732> (1985).
42. Guazzelli, É. & Pouliquen, O. Rheology of dense granular suspensions. *Journal of Fluid Mechanics* **852**, 852–925 (2018).
43. Wilson, H. J. An analytic form for the pair distribution function and rheology of a dilute suspension of rough spheres in plane strain flow. *Journal of Fluid Mechanics* **534**, 97–114 (2005).
44. Wilson, H. J. & Davis, R. H. The viscosity of a dilute suspension of rough spheres. *Journal of Fluid Mechanics* **421**, 339–367 (2000).
45. Rampall, I., Smart, J. R. & Leighton, D. T. The influence of surface roughness on the particle pair distribution function of dilute suspensions of non-colloidal spheres in simple shear flow. *Journal of Fluid Mechanics* **339**, 1–24 (1997).
46. Milner, S. T. Hydrodynamics of semidilute polymer solutions. *Phys. Rev. Lett.* **66**, 1477–1480 (1991).
47. Onuki, A. Elastic Effects in the Phase Transition of Polymer Solutions under Shear Flow. *Phys. Rev. Letts.* **62**, 2472–2475 (1989).
48. Foss, D. R. & Brady, J. F. Structure, Diffusion and Rheology of Brownian Suspensions by Stokesian Dynamics simulation. *Journal of Fluid mechanics* **407**, 167–200 (2000).
49. Boyer, F., Guazzelli, É. & Pouliquen, O. Unifying Suspension and Granular Rheology. *Physical Review Letters* **107**, 188301, <https://doi.org/10.1103/PhysRevLett.107.188301> (2011).
50. Miller, R. M. & Morris, J. F. Normal stress-driven migration and axial development in pressure-driven flow of concentrated suspensions. *Journal of Non-Newtonian Fluid Mechanics* **135**, 149–165, <https://doi.org/10.1016/j.jnnfm.2005.11.009> (2006).
51. Chan, N. Y., Chen, M. & Dunstan, D. E. Elasticity of Polymer Solutions in Couette Flow measured by Fluorescence Resonance Energy Transfer (FRET). *European Physical Journal E* **30**, 37–41 (2009).
52. Chan, N. Y., Chen, M., Hao, X.-T., Smith, T. A. & Dunstan, D. E. Polymer Compression in Shear Flow. *The Journal of Physical Chemistry Letters* **1**, 1912–1916, <https://doi.org/10.1021/jz100535b> (2010).
53. Mavrantzas, V. G. & Beris, A. N. Modeling of the rheology and flow-induced concentration changes in polymer solutions. *Phys. Rev. Lett.* **69**, 273–276 (1992).
54. Dixon, P. K., Pine, D. J. & Wu, X.-L. Mode Selection in the Dynamics of Sheared Polymer Solutions. *Phys. Rev. Lett.* **68**, 2239–2242 (1992).
55. Barnes, H. A., Hutton, J. F. & Walters, K. *An Introduction to Rheology*. (Elsevier, Amsterdam, 1989).
56. Stratton, R. A. The dependence of non-Newtonian viscosity on molecular weight for “Monodisperse” polystyrene. *Journal of Colloid and Interface Science* **22**, 517–530 (1966).
57. Morris, J. F. Shear Thickening of Concentrated Suspensions: Recent Developments and Relation to Other Phenomena. *Annual Review of Fluid Mechanics* **52**, 121–144, <https://doi.org/10.1146/annurev-fluid-010816-060128> (2020).

## Acknowledgements

DD would like to thank Professor George Franks for constructive discussion and listening *ad infinitum*.

## Author contributions

D.E.D. wrote the main manuscript text. D.J.E.H. did the simulations and prepared the figures. Both authors contributed to the intellectual content and reviewed the manuscript.

## Competing interests

The authors declare no competing interests.

## Additional information

**Correspondence** and requests for materials should be addressed to D.E.D.

**Reprints and permissions information** is available at [www.nature.com/reprints](http://www.nature.com/reprints).

**Publisher’s note** Springer Nature remains neutral with regard to jurisdictional claims in published maps and institutional affiliations.



**Open Access** This article is licensed under a Creative Commons Attribution 4.0 International License, which permits use, sharing, adaptation, distribution and reproduction in any medium or format, as long as you give appropriate credit to the original author(s) and the source, provide a link to the Creative Commons license, and indicate if changes were made. The images or other third party material in this article are included in the article's Creative Commons license, unless indicated otherwise in a credit line to the material. If material is not included in the article's Creative Commons license and your intended use is not permitted by statutory regulation or exceeds the permitted use, you will need to obtain permission directly from the copyright holder. To view a copy of this license, visit <http://creativecommons.org/licenses/by/4.0/>.

© Crown 2020